ISSN: 2414-1895 DOI: 10.6919/ICJE.202404_10(4).0004

Finite Element Analysis of Solid Rocket Motor Grain under Horizontal Storage

Yanshen Zhang[a], Hongfu Qiang[b], and Xueren Wang[c]

Rocket Force University of Engineering, Xi'an 710025, China

[a]zys9232@126.com, [b]Qiang@163.com, [c]Alittlepanda@163.com

Abstract

This study proposes a finite element calculation method for solid propellant considering damage based on thermal viscoelastic constitutive theory and cumulative damage theory. The proposed method is used to analyze the mechanical response and damage law of the solid rocket motor (SRM) under horizontal storage conditions. In the considered scenario, rocket motor is thought to be exposed to storage during its lifetime, which provoke stress and strain in the propellant grain. Research has shown that under horizontal storage conditions, the grain undergoes shrinkage due to solidification and cooling, and significant thermal stress is generated at the mesoporous position; The front and rear ends of the grain experience slight sagging under the action of gravity; Under the combined influence of solidification cooling and gravity, there is local stress concentration at the root of the stress release boot. Cumulative damage is combined with the material response to investigate the effect of periodic flipping on the propellant grain. The accumulated damage values with respect to loads show that flipping can avoid the same position of the propellant grain being in a stress concentration state for a long time, thereby preventing the rapid accumulation of damage and having a positive impact on extending the service life of the SRM. For solid motors with stress release boot structures, the propellant grain near the root of the stress release boot is more likely to be damaged during storage, which requires special attention. Preliminary analysis results show that the different flipping cycles have little effect on the distribution pattern of the damage, but further research is needed to address this issue.

Keywords

Solid Rocket Motor; Solid Propellant; Grain; Finite Element Method; Cumulative Damage.

1. Introduction

The solid rocket motor(SRM)is generally subjected to different types of loads from the completion of casting to the end of its combustion task, such as gravity, propellant solidification and cooling, temperature fluctuations, long-term storage, vibration caused by vehicle transportation, pressure, and acceleration during ignition and flight [1]. These loads can result in changes in temperature, displacement, strain, and stress of the grain, potentially leading to interface debonding, grain creep, grain dewetting, and crushing. All of these will compromise the structure integrity of the motor and even cause serious accidents [2,3].

Some scholars have conducted research on the mechanical response and structural integrity of the propellant grain structures under different loads. Chyuan [4] considered propellants as a linear thermo viscoelastic material and studied the effect of different thermal load histories on the structure of the propellant grain through finite element method. Subsequently, Chyuan [5] used dynamic analysis methods to study the mechanical response of propellant grains during motor ignition. Okan Yilmaz

ISSN: 2414-1895 DOI: 10.6919/ICJE.202404_10(4).0004

et al. [6] further established a harmonic function of thermal load on time, studied the load changes of SRMs in multiple states of sea, land, and air, and obtained the limit state function of motor structural failure. There are also some literature studies on the mechanical characteristics and structural integrity of SRMs under transportation vibration, temperature changes, ejection, and ignition conditions [7-13].

When the SRM is in a horizontal storage state, the propellant grain is mainly subjected to solidification cooling load and gravity load. Due to the viscoelastic properties of solid propellants, under the action of self weight load, as shown in Figure 1, the propellant grain will undergo creep deformation, port deformation and sinking, affecting the gas discharge process and even blocking the motor nozzle. In addition, the storage time of the SRM can reach several decades, and minor structural damage inside the propellant grain will continuously weaken its load-bearing capacity under load, damaging its structural integrity. Therefore, in the horizontal storage state, the motor can adopt a periodic flipping storage strategy to eliminate the creep deformation of the grain, alleviate local large stress and strain, and reduce grain damage.

Tang et al. [14] analyzed the displacement level of the SRM structure under long-term self weight load under horizontal storage conditions, and believed that a turnover period of six months can effectively eliminate the accumulation of creep in the grain; Yang et al. [15] obtained the stress at the dangerous interface of the grain under vacuum, high pressure, and actual storage conditions through numerical calculations. However, neither of the above studies considered the problem of slow accumulation of the grain damage in long-term storage environments. At present, there is relatively little research on the damage analysis of solid propellant grains under periodic flipping conditions during horizontal storage.

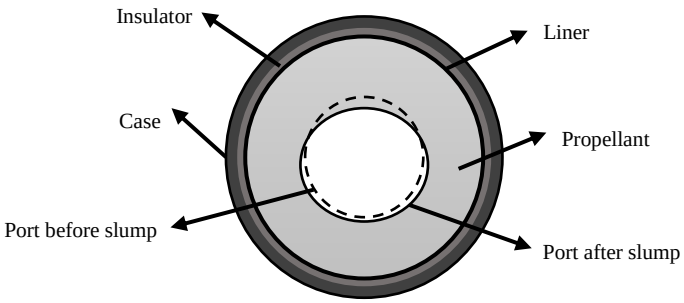

Figure 1. Schematic of grain deformation when the SRM is stored in horizontal position

2. Finite Element Method

Before conducting finite element calculations, it is necessary to first use appropriate material constitutive models based on the calculation object. The solid propellant studied in this article adopts a composite solid propellant of butadiene and hydroxylamine, which is a high molecular weight polymer containing high filling solid particles such as inorganic oxidants and metal additives, and the matrix is an adhesive matrix. Its mechanical properties mainly depend on the polymer adhesive, so the mechanical properties of the solid propellant mainly exhibit viscoelasticity.

2.1 Thermoviscoelastic Constitutive Relationship

When the propellant is subjected to a small load, there is almost no internal damage, therefore, the deformation at this time can be described using a linear viscoelastic constitutive model. The general form of the three-dimensional constitutive equation for linear viscoelastic materials is as follows:

$$\sigma_{ij}(t) = S_{ij}(t) + \frac{1}{3}\delta_{ij}\sigma_{kk}(t) \tag{1}$$

ISSN: 2414-1895 DOI: 10.6919/ICJE.202404_10(4).0004

$$S_{ij}(t)=\frac{1}{1+\nu}\int_{-\infty}^{t}E(\xi-\xi')\frac{\partial e_{ij}(\tau)}{\partial\tau}\mathrm{d}\tau \tag{2}$$

$$\sigma_{kk}(t)=\frac{1}{1-2\nu}\int_{-\infty}^{t}E(\xi-\xi')\frac{\partial \hat{\varepsilon}_{kk}(\tau)}{\partial\tau}\mathrm{d}\tau \tag{3}$$

Where, E(t) is the relaxation modulus of the material, $S_{ij}(t)$ and $\sigma_{kk}(t)$ represent the deviatoric stress and spherical stress respectively. $\hat{\varepsilon}_{kk}=\varepsilon_{kk}-3\alpha\theta$, e_{ij} and ε_{kk} represent the deviatoric stress and spherical stress, α is the thermal coefficient of expansion, θ represents the variation of temperature, ξ and ξ' are the reduced time, and their forms are as follows:

$$\xi=\xi(t)=\int_0^t\frac{\mathrm{d}t'}{a_T[T(t')]},\quad \xi'=\xi'(\tau)=\int_0^\tau\frac{\mathrm{d}t'}{a_T\left[T(t')\right]} \tag{4}$$

Where, a_T the temperature shift factor. In order to describe the effect of temperature on the shift factor, the WLF equation is used, and the function is defined as:

$$\lg a_T=\frac{-C_1(T-T_r)}{C_2+(T-T_r)} \tag{5}$$

Where, C_1 and C_2 are material constants, T is the current temperature, T_r is the reference temperature.

2.2 Damage Model of the Grain

During the storage process, the structure of solid rocket motor propellant will slowly change under long-term loads, resulting in a decrease in the mechanical properties of the propellant grain. This is a process of damage accumulation. When the damage develops, obvious cracks will appear, leading to the failure of the charge. Miner [16] was the first to propose the concept of cumulative damage. When studying the damage of metal materials under cyclic loading, he proposed a linear cumulative damage model:

$$D=\sum_{i=1}^{n}\frac{\Delta t_i}{t^*(\sigma_i)} \tag{6}$$

Where $t^*(\sigma_i)$ is the fail time of the materials under the stress level of σ_i, D is the damage parameter of the material.

Experiments conducted by Laheru [17] indicate that the cumulative damage rule may be useful in the prediction of service life of solid propellants. Some studies that were related to the case-bonded solid propellant grain structural integrity analysis [2, 4, 7] discussed cumulative damage as a theoretical possibility. It has also been shown that a power function will describe the relationship between applied constant stress and reduced time to failure:

$$\frac{t^*(\sigma_i)}{t^*(\sigma_0)}=\left(\frac{\sigma_0}{\sigma_i}\right)^{\beta} \tag{7}$$

ISSN: 2414-1895 DOI: 10.6919/ICJE.202404_10(4).0004

According to the damage evolution model, the relationship between propellant loading stress, loading time, and damage can be obtained by integrating equation(6):

$$D = \frac{1}{N}\left[\int_0^t \sigma(t)^{\beta}\,\mathrm{d}t\right]^{1/\beta} \tag{8}$$

Where, β is the exponential of cumulative damage, N is Lebesgue stress norm, and its form is as follows:

$$N = \sigma_0 t_0^{1/\beta} \tag{9}$$

Where, σ_0 is the reference creep stress, t_0 is the corresponding failure time.

2.3 Incremental Finite Element Form

For the structural finite element analysis of the constitutive equation of viscoelastic materials, the mechanical response is not only related to the current load state, but also closely related to the entire load action history. Therefore, this type of problem generally needs to be solved using the incremental method. Firstly, discretize the constitutive model and divide the time interval [0, t] into several analysis time steps, namely:

$$[0,t] = \cup_n [t_{n-1}, t_n], \quad t_n = t_{n-1} + \Delta t_n \tag{10}$$

Similarly, reduced time ξ(t) and the damage variable D(t) are also divided into corresponding time steps:

$$[0,\xi] = \cup_n [\xi_{n-1}, \xi_n], \quad \xi_n = \xi_{n-1} + \Delta\xi_n \tag{11}$$

$$[0,D] = \cup_n [D_{n-1}, D_n], \quad D_n = D_{n-1} + \Delta D_n \tag{12}$$

The discretized constitutive equation can be obtained:

$$\Delta\sigma_{ij}(t_m) = \Delta S_{ij}(t_m) + \frac{1}{3}\delta_{ij}\Delta\sigma_{kk}(t_m) \tag{13}$$

$$\Delta S_{ij}(t_m) = S_{ij}(t_m) - S_{ij}(t_{m-1}) \tag{14}$$

$$\Delta\sigma_{kk}(t_m) = \sigma_{kk}(t_m) - \sigma_{kk}(t_{m-1}) \tag{15}$$

At the end of each time step, the viscoelastic strains $\Delta S_{ij}(t_m)$ and $\Delta\sigma_{kk}(t_m)$ can be obtained by integrating the corresponding strain rate:

$$\varepsilon_{ve}^n = \varepsilon_{ve}^{n-1} + [(1-\beta)\frac{\mathrm{d}\varepsilon_{ve}^n}{\mathrm{d}t}|_{n-1} + \beta\frac{\mathrm{d}\varepsilon_{ve}^n}{\mathrm{d}t}|_n]t_n \tag{16}$$

ISSN: 2414-1895 DOI: 10.6919/ICJE.202404_10(4).0004

Assuming that the stress varies linearly at each time step, D(t) can be obtained from Equation 9:

$$D_n = D_{n-1} + \frac{1}{N}\left\{\int_{t_{n-1}}^{t_n}\left[\sigma_{n-1} + \frac{\Delta\sigma_n}{\Delta t_n}\left(t - t_{n-1}\right)\right]^{\beta} \mathrm{d}t\right\}^{1/\beta} \tag{17}$$

3. Numeration Model

3.1 Geometric and Finite Element Models of Solid Rocket Motors

The storage process of a SRM can be analyzed using a three-dimensional model. In this model, the motor initially cools down from 331.15K to 298.15K and maintains this temperature for a period of time. Afterward, the motor is placed horizontally for a year of storage. The model, shown in Figure 2, is built in Abaqus and has dimensions of 4200mm in length, 1800mm in outer diameter, and 500mm in inner diameter. The motor consists of a shell, an insulator, and a propellant grain. Stress release boots are present inside the insulator at the front and rear of the motor. Several simplifications were made in the modeling process considering the complex structure of the motor. These simplifications include omitting the structure of the front and rear frame and motor nozzle, assuming tight bonding between the shell and the grain, and neglecting the presence of gas in the middle. The calculation process does not account for interface debonding. As shown in Figure 3,the built motor's finite element model consists of 227,600 elements and 248,862 nodes.

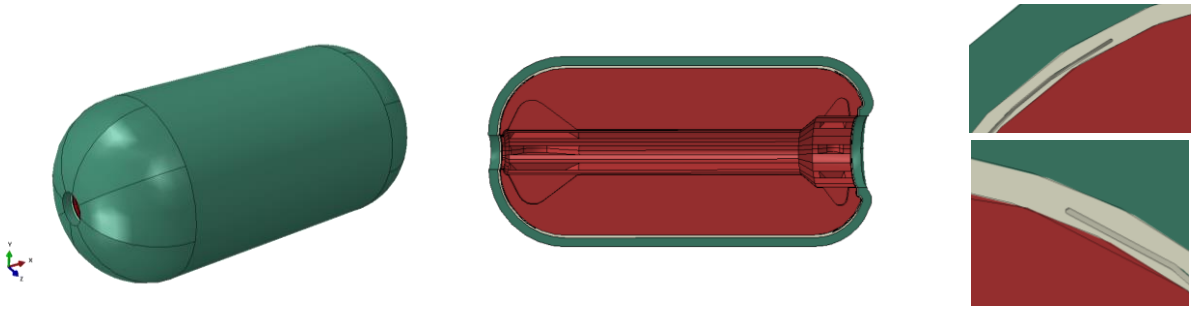

(a) Whole structure (b) Section structure (c) Local structure

Figure 2. Schematic diagram of the SRM

Figure 3. Finite element model of the SRM

3.2 Material Properties

The case and insulation layer adopt the linear elastic material model, and the propellant grain adopt the viscoelastic material model. The material properties of the case, insulation layer, and propellant grain are shown in Tables 1 and 2:

ISSN: 2414-1895 DOI: 10.6919/ICJE.202404_10(4).0004

Table 1. Three Scheme comparing

Parts	Elastic modulus/MPa	Poisson's ratio	Density/ (g/cm3)	Thermal expansion coefficient/ ℃-1
Case	210000	0.3	7.8	1.1e-5
Insulation	6.2	0.495	1.1	9.8e-5
Grain	E(t)	0.49	1.7	9.25e-5

Table 2. Relaxation modulus of propellant grain

i	τ_i/s	E_i/Mpa
∞	—	0.6468
1	1	5.943
2	10	1.438
3	100	1.307
4	1000	0.8172
5	10000	0.5452
6	100000	0.4266

The zero stress temperature of the propellant is 331.15K, and the WLF equation coefficients C1=20.804 and C2=458.987 are taken as the reference temperature Tr=298.15K.

The damage parameters of the propellant can be obtained through the propellant constant tensile failure experiment to obtain the failure time of propellant specimens at different stress levels, which can be fitted using Equation 9. In this calculation β= 5.455, N=3.514.

3.3 Loading Conditions

During horizontal storage of the SRM, it is crucial to account for the combined impact of temperature load and gravity load. Firstly, the SRM undergoes a gradual cooling process from its initial zero stress temperature of 331.15K to 298.15K, maintaining this temperature for a continuous period of 72 hours before being placed horizontally. The orientation of both gravity and the SRM flipping direction are illustrated in Figure 4. The flipping process involves a 90-degree rotation along the motor's central axis when viewed from the motor's head to tail, occurring at the conclusion of each flipping cycle. This results in the motor's I-IV quadrant being successively positioned towards the vertical downward gravity orientation, with this cycle repeated intermittently during storage.

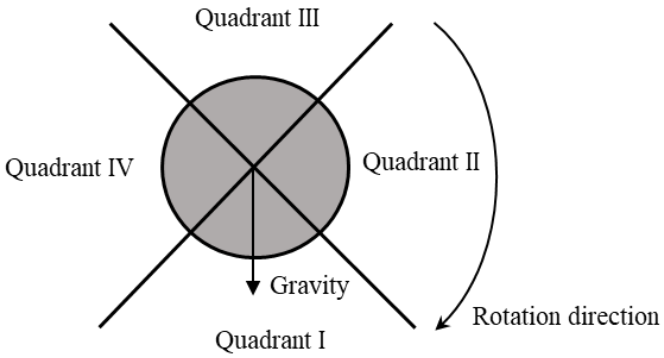

Figure 4. Rotation direction of solid motor

ISSN: 2414-1895 DOI: 10.6919/ICJE.202404_10(4).0004

4. Analysis of Numerical Results

Table 3 displays six different conditions established based on the storage time and flipping cycle of the solid motor. Condition 1 involves storing the SRM without flipping for six months, aiming to examine the mechanical response pattern of the motor grain when stored horizontally. Conditions 2 and 3 entail the storage of the SRM for two years under non-flipping and periodic flipping scenarios. The resulting numerical data is utilized to evaluate the influence of flipping on the propellant grain's damage. Conversely, conditions 4 to 6 involve storing the SRM for eight years under varying flipping cycle conditions. Subsequently, the numerical findings are employed to probe the impact of the flipping cycle on the damage mechanism of the propellant grain.

Table 3. Patameter setting under different conditions

Condition	Flipping cycle(T_t)/a	Storage time(T_s)/a
1	-	0.5
2	-	2
3	0.5	2
4	0.5	8
5	1	8
6	2	8

4.1 Mechanical Response of the Grain under Horizontal Storage Conditions

Figure 5 (a) depicts the axial displacement distribution of the motor following six months of horizontal storage, after condition 1 calculations were made. Notably, a significant displacement is observed at the front and rear ends of the propellant grain, with the movement direction oriented towards the middle hole. The maximum displacement recorded is 23.47mm, representing approximately 0.56% of the motor length. In Figure 5 (b), the vertical displacement distribution of the motor is illustrated, highlighting an enlargement in the pore size at the middle hole due to the solidified cooling propellant shrinkage. The displacement direction of the propellant's front and rear ends is downward, attributed to gravitational sagging. Specifically, the maximum sagging displacement measured is 10.59mm, accounting for around 0.59% of the motor diameter.

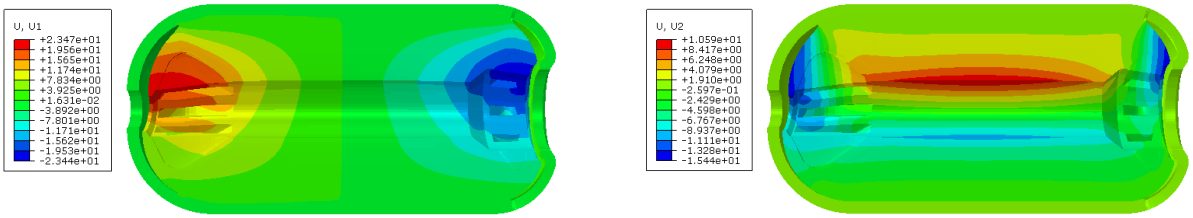

(a) axial displacement (b) vertical displacement

Figure 5. Cloud picture of displacement

After six months of horizontal storage, the Mises stress distribution on the outer surface of the propellant grain is illustrated in Figure 6. The area with relatively high stress levels can be observed near the stress release boot position at the front and rear ends of the upper outer surface of the propellant grain, as shown in Figure 6 (a). In the third quadrant of the propellant grain, the highest equivalent stress is recorded at the position of stress release boot at the front end, reaching 0.787 MPa. This heightened stress level can be attributed to the significant difference in expansion coefficients

ISSN: 2414-1895 DOI: 10.6919/ICJE.202404_10(4).0004

between the propellant grain and the shell. Upon a decrease in temperature, the propellant grain experiences tensile forces near the root of the stress release boot, resulting in stress concentration. Moreover, at the stress release boot position in the third quadrant, the propellant grain is subjected to tensile forces under gravity load, leading to stress concentration due to load superposition at that location. Furthermore, Figure 6 (b) displays the local Mises stress distribution at the front end of the propellant grain, indicating that the high-stress area is primarily located on the surface of the propellant grain, showing a circumferential distribution along the root position.

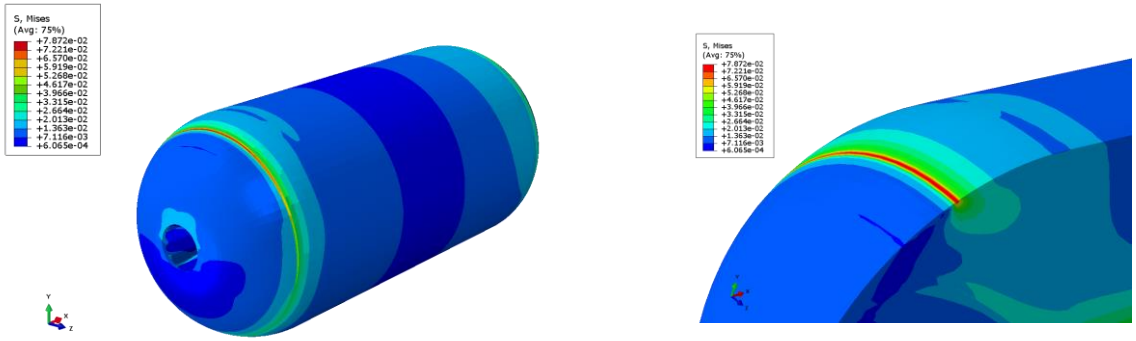

(a) Mises stress distribution of the whole structure

(b) Mises stress distribution of the front local structure

Figure 6. Mises stress distribution of the grain after horizontally storing for 0.5 a

Figure 7 shows the Mises stress distribution along the XOY symmetry plane profile of the propellant grain after six months of horizontal storage. It is evident from the figure that, apart from the front and rear root removal positions, the inner surface of the middle hole of the propellant grain experiences significantly elevated stress levels overall. Specifically, the maximum Mises stress recorded at the center of the inner surface reaches 0.0408 MPa. This heightened stress is primarily attributed to the thermal stress resulting from the propellant grain's contraction during the cooling phase.

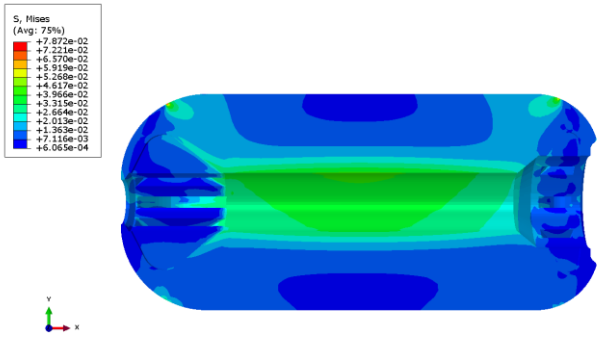

Figure 7. Mises stress distribution of propellant grain profile after the horizontal storage of 0.5a

In this article, the correlation between damage accumulation and the stress history of the propellant grain in the cumulative damage model necessitates a detailed analysis of the stress distribution law. To accomplish this, paths 1-3 on the inner surface of the propellant grain were selected for stress distribution analysis, as depicted in Figure 8 (a). The stress distribution along these paths is illustrated in Figure 9 (a), where it is evident that under horizontal storage conditions, path 1 - the inner hole path in the third quadrant - exhibits relatively high stress levels. Specifically, the maximum value recorded is approximately 0.0408 MPa at 2160 mm, suggesting that the inner hole stress is primarily induced by solidification, with the gravity load impact being relatively minimal.

ISSN: 2414-1895 DOI: 10.6919/ICJE.202404_10(4).0004

Moving to the outer surface of the propellant grain, Figure 8 (b) illustrates the stress distribution along paths 4-6. The analysis reveals that while stress levels along path 2 are mostly below 0.02 MPa, peaks are observed at 790 mm and 4136 mm. Notably, stress concentrations at the root of the stress release boot in the three quadrants of path 4 are measured at 0.0787 MPa and 0.0648 MPa, respectively. Differences in stress concentration are observed in path 5 and path 6, indicating a complex interplay between solidification cooling and gravity load effects which can either reinforce or counterbalance each other. These findings are corroborated by numerical results referenced in [12].

The analysis indicates that the main stress concentration zone is situated at the root of the front of the three-quadrant propellant grain. Considering that each quadrant may occupy the position of the three-quadrant when the SRM is inverted during storage, further investigation into stress levels in the circular area at the front of the stress release boot is imperative. Selecting path 7 for analysis, as depicted in Figure 8 (c), the Mises stress level distribution curve of the propellant grain along this path is shown in Figure 9 (c). Stress levels are highest near the stress release boot in quadrant III, reaching 0.0787 MPa, while the minimum stress level is observed in the middle of quadrant I, at 0.0263 MPa.

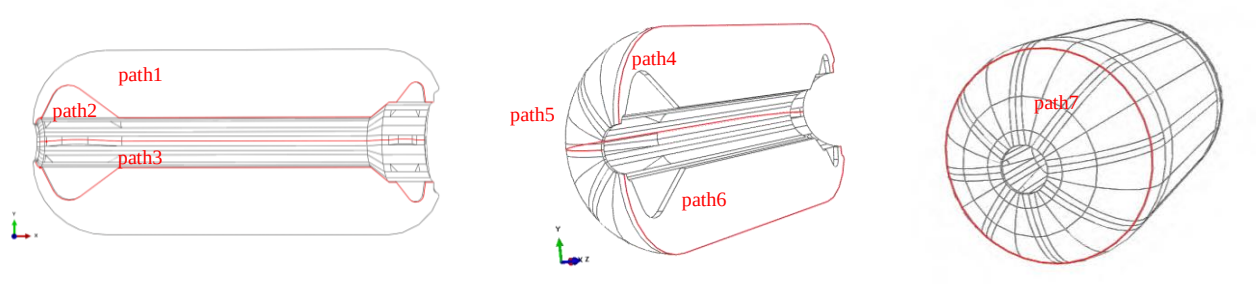

(a)path1-3 (b)path4-6 (c)path7

Figure 8. The distribution position of characteristic lines of propellant grain

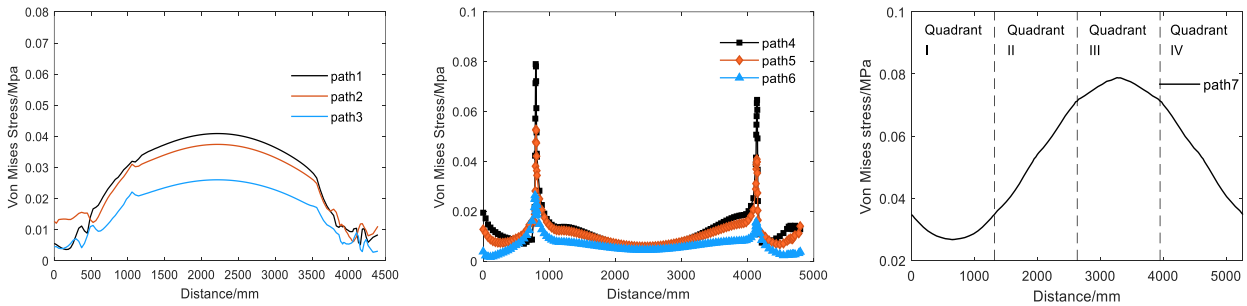

(a) path1-3 (b) path4-6 (c)path7

Figure 9. Curves of path distance vs. Mises stress of propellant grain

After a thorough analysis, it is evident that the stress level is notably high at the root position of the propellant grain's front end under horizontal storage conditions, leading to the most severe damage accumulation during storage. Special attention is needed in this regard.

4.2 The Effect of Regular Flipping on the Damage of the Grain

The damage situation of the grain was analyzed using the numerical results from conditions 2 and 3 in Table 3. After 2 years of horizontal storage without flipping, the distribution of the grain damage field is illustrated in Figure 10 (a). The area with greater damage is located at the root of the stress release boot at the front end of the third quadrant grain, displaying a circumferential distribution. The maximum cumulative damage value observed in this area is 6.22%. On the other hand, Figure 10 (b)

ISSN: 2414-1895 DOI: 10.6919/ICJE.202404_10(4).0004

displays the damage field distribution of the propellant grain after two years of horizontal storage with a turnover period of six months. Notably, the larger cumulative damage area is observed in a circular pattern along the root of the stress release boot at the front end of the propellant grain. Specifically, the maximum cumulative damage in this area is 1.93%, which accounts for 31.0% of the maximum damage observed in the propellant under the condition of no flipping.

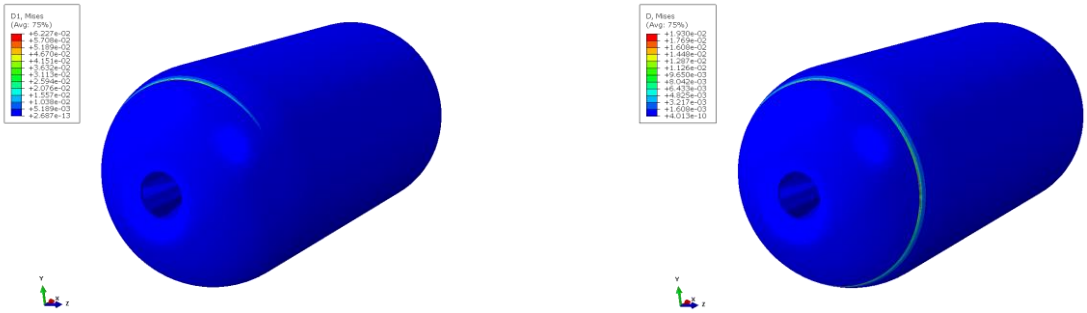

(a) Unturned motor (b) Periodic flipped motor

Figure 10. Cumulative damage distribution of propellant grain after the horizontal storage of 2 years

Further analysis was conducted on the damage of solid propellants at the root position of the front end of the grain. The distribution curve of the propellant grain damage along path 7 after horizontal storage for 2 years is shown in Figure 11. It is evident from the figure that without flipping, the propellant grain sustains the most damage in quadrant III, reaching a maximum of 6.23% after 2 years. In contrast, damage in quadrants II and IV is relatively minimal, varying from 0.07% to 3.58%, while damage in quadrant I is negligible, staying within 0.07%. When adopting the storage condition of flipping for half a year, the damage to the propellant grain is evenly distributed across all quadrants after 2 years, with damage values ranging from 1.73% to 1.93%. This observation suggests that regular flipping can mitigate the accumulation of damage in the local stress concentration position of the propellant grain, thereby averting premature damage to the structural integrity of the propellant grain.

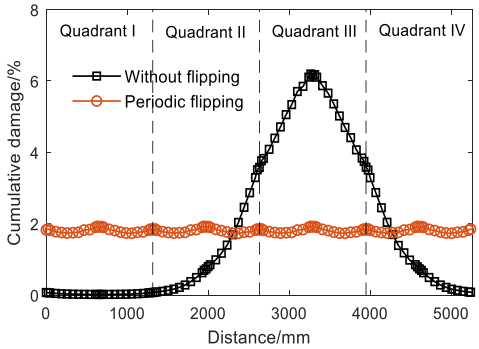

Figure 11. Curves of path distance vs. cumulative damage of propellant grain on path3 after the horizontal storage of 2a

Figure 12 illustrates the damage change curves at the maximum damage point of the propellant grain under horizontal storage conditions over a 2-year period. In the absence of flipping, the figure reveals a nearly linear increase in cumulative damage value with the passage of storage time. This consistent rise can be attributed to the relatively stable stress level experienced by the propellant grain during storage. Conversely, when subjected to a six-month flipping cycle, the cumulative damage at the maximum damage point escalated to 1.56% following the completion of the initial flipping cycle,

ISSN: 2414-1895 DOI: 10.6919/ICJE.202404_10(4).0004

with subsequent gradual growth observed in the subsequent three flipping cycles, ultimately reaching 1.93% after the 2-year period.

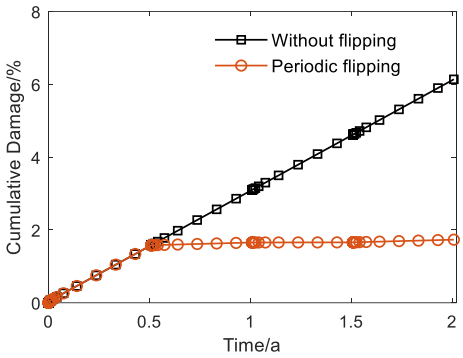

Figure 12. Cumulative damage curves of maximum damage point of propellant grain vs. time in the horizontal storage of 2a

4.3 The Effect of Flipping Cycle on the Damage of the Grain

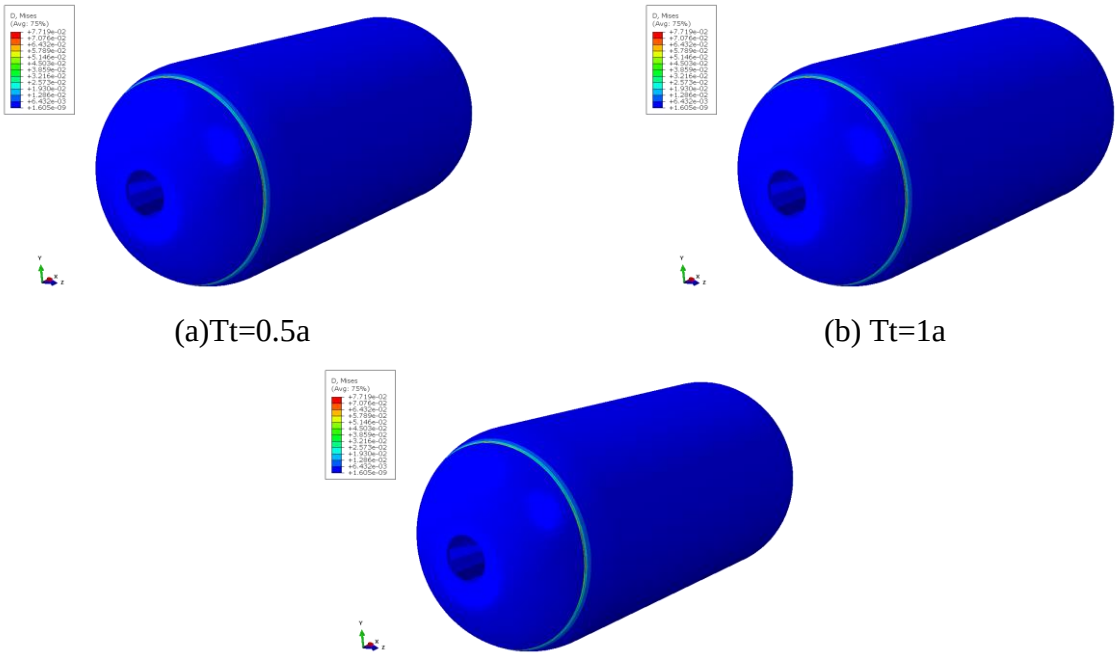

(a)Tt=0.5a (b) Tt=1a

(c) Tt=2a

Figure 13. Cumulative damage distribution of propellant grain after the horizontal storage of 8 years

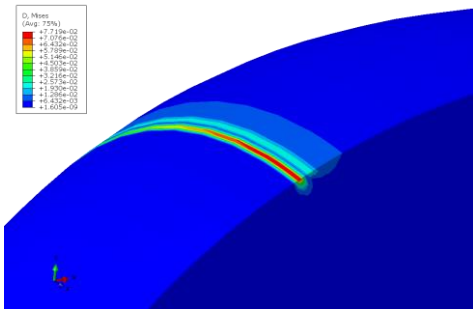

Figure 14. Cumulative damage distribution of propellant grain profile after the horizontal storage of 8a

ISSN: 2414-1895 DOI: 10.6919/ICJE.202404_10(4).0004

Analysis was conducted to study the impact of flipping cycles on the cumulative damage of horizontally stored propellant grain. The load parameters corresponding to conditions 4-6 in Table 3 were considered for the investigation. The cumulative damage distribution of the propellant grain after 8 years of horizontal storage was examined with flipping cycles of six months, one year, and two years, as depicted in Figure 13. The figure illustrates that across various flipping cycle conditions, the pattern of propellant grain damage distribution remains largely consistent. The region with higher cumulative damage is observed in a circular configuration along the front end of the propellant grain, with the maximum damage point concentrated at the front end, representing 7.71% damage. Furthermore, Figure 14 displays the cumulative damage distribution along the XOY symmetry plane of the propellant grain, revealing that the areas with greater cumulative damage are predominantly situated at the root of detachment on the outer surface of the propellant grain. Comparing the damage distribution patterns under different flipping cycle storage conditions, it is evident that there is significant similarity in the distribution of damage across the propellant grain.

Figure 15 illustrates the cumulative damage over time curve at the maximum damage point of the propellant grain stored horizontally for 8 years, under various flipping cycles. In the initial 2 years of horizontal storage, the propellant grain exhibited different levels of maximum damage accumulation across flipping cycles. Specifically, with a 2-year flipping cycle, the maximum damage reached 6.24%, whereas for 1-year and half-year flipping cycles, the maximum damage values were 3.49% and 1.96%, respectively. As the storage period extended to 4 years, the maximum damage values increased for propellant grains subjected to different flipping cycles. The values were 6.97%, 3.90%, and 3.90% for 2-year, 1-year, and half-year flipping cycles, respectively. Remarkably, after 8 years of horizontal storage, the maximum damage values remained consistent at 7.71% for all three flipping cycle durations. The observed pattern of damage accumulation can be attributed to the stress distribution within the propellant grain during horizontal storage. Initially, when the flipping cycle is longer, the front end of the propellant grain experiences prolonged high stress at the detachment root in the third quadrant of the Solid Rocket Motor (SRM), leading to faster damage accumulation. Conversely, shorter flipping cycles result in frequent changes in gravity load and internal stress distribution, slowing down the maximum damage accrual in the propellant grain. Ultimately, at the conclusion of the 8-year storage cycle, propellant grains subjected to flipping cycles of six months, one year, and two years displayed nearly identical cumulative damage values at the maximum damage point, indicating the convergence of damage accumulation despite initial variations.

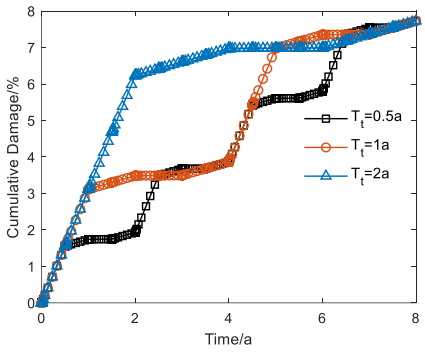

Figure 15. Curves of cumulative damage of maximum damage point of propellant grain vs. time in the horizontal storage of 8 years

5. Conclusion

This study proposes a finite element calculation method for solid rocket motor grain considering damage based on thermal viscoelastic constitutive theory and cumulative damage theory. And the mechanical response and damage law of the SRM under horizontal storage conditions were analyzed. Research has shown that under horizontal storage conditions, the propellant grain undergoes

ISSN: 2414-1895 DOI: 10.6919/ICJE.202404_10(4).0004

shrinkage due to solidification and cooling, and significant thermal stress is generated at the mesoporous position; The front and rear ends of the propellant grain experience slight sag under the action of gravity. Under the combined influence of solidification cooling and gravity, there is local stress concentration at the root of the stress release boot. Cumulative damage is combined with the material response to study the effect of periodic flipping on solid motor propellant grains. The accumulated damage values with respect to loads show that flipping can avoid the same position of the propellant grain being in a stress concentration state for a long time, thereby preventing the rapid accumulation of damage and having a positive impact on extending the service life of the SRM. Regularly flipping the motor can help prevent rapid accumulation of damage by avoiding long-term stress concentration at the same position of the propellant, thereby extending the service life of the SRM. It is important to note that for solid motors with stress release boot structures, special attention should be paid to the propellant grain near the root of the stress release boot, as it is more susceptible to damage during storage. Although the impact of different flipping cycles on the distribution pattern of propellant damage is not significant, further research is needed to fully address this issue. These findings offer valuable insights for assessing the effects of periodic flipping on the horizontal storage of solid rocket motor propellant grains.

References

[1] K. Chen, Q. Ren, J. Cheng, et al. Structural response analysis of a solid rocket motor with HTPB propellant grain under vertical storage condition. Journal of Northwestern Polytechnical University, Vol. 40 (2022) No. 1, p.49-52.

[2] R.A. Heller, M.P. Singh, H. Zibdeh. Environmental Effects on Cumulative Damage in Rocket Motors, Journal of Spacecraft & Rockets, Vol. 22 (2015) No. 2, p.149-155.

[3] R. Marimuthu, B.N. Rao. Development of efficient finite elements for structural integrity analysis of solid rocket motor propellant grains, International Journal of Pressure Vessels and Piping, Vol. 111 (2013), p.131-145.

[4] S.W. Chyuan. Chyuan. A Study of Loading History Effect for Thermoviscoelastic Solid Propellant Grains, Computers and Structures, Vol. 77 (2000) No.6, p.735-745.

[5] S.W. Chyuan. Dynamic analysis of solid propellant grains subjected to ignition pressurization loading, Journal of Sound and Vibration, Vol. 268 (2003) No.3, p.465-483.

[6] Okan Yilmaz. Reliability Assessment of Solid-Propellant Rocket Motors Under Storage and Transportation Loads, Journal of Spacecraft and Rockets, Vol. 54 (2003) No.6, p.1356-1366.

[7] B. Lu, Z.T. An, T.P. Li. Research Status of Structural Stability of Solid Rocket Engine, Journal of Ordnance Equipment Engineering Vol. 42 (2021) No.2, p244-247.

[8] Y.L. Liu, T.P. Li, Z.T. An. Numerical Analysis of Vehicle and Missile Solid Rocket Motor Response under Road Transportation Environment, Journal of Academy of Armored Force Engineering, Vol. 32 (2018) No. 4, p. 45-50.

[9] B.Q. Xu, M.Z. Lu, G.C. Li, et al. Study on Damage of Solid Rocket Motor Bonding Interface Caused by Temperature and Vibration Load During Vehicle Transportation, Vol. 42 (2021) No. 07, p. 252-257.

[10] B. Deng, D. Yang, J.B. Duan, et al. Cumulative Damage Analysis of Solid Rocket Motor Grain under Temperature Loading, Journal of Propulsion Technology, Vol. 34 (2013) No. 2, p. 280-284.

[11] Y.F. Wang, Y.G. Xing, G.C. Li, et al. Stress and Cumulative Damage of Solid Charge Under Temperature Cycling Condition, Journal of System Simulation, Vol. 24 (2012) No. 5, p. 1132-1137.

[12] L.F. Jia, H.B. Shi, B.L. Sha, et al. Dynamic Response of Solid Rocket Motor Grain-Liner Interface under Flip Condition, Journal of Propulsion Technology, Vol. 43 (2022) No. 12, p. 395-401.

[13] B Long, X.L. Chang, J.W. Lai, et al. The Structure Analysis of Solid Propellant Motor under Temperature Load, Journal of Projectiles, Rockets, Missiles and Guidance, Vol. 31 (2011) No. 2, p. 130-132.

[14] G.J. Tang, D.C. Yuan, J.T Li, et al. Displacement analysis of solid motor grain under long-time gravity load, Journal of Solid Rocket Technology, Vol 30 no 6 Vol. 30 (1) No. 6, p. 482-485.

[15] Y.C. Yang, N. Zhang, H.F. Qiang, et al. Interface Stress Analysis of SRM under Horizontal Storage State, Aerospace Shanghai, Vol. 3 (2007) No. 1, p. 50-53.

ISSN: 2414-1895 DOI: 10.6919/ICJE.202404_10(4).0004

[16] Miner M A. Cumulative Damage in Fatigue, Journal of Applied Mechanics, Vol. 12 (1945) No. 3, p. 159-164.

[17] K.L. Laheru. Development of a generalized failure criterion for viscoelastic materials, Journal of Propulsion and Power, Vol. 298(1992), p.756-759.